Exp Brain Res (2007) 181:87–98
DOI 10.1007/s00221-007-0908-1

RESEARCH ARTICLE

Spectral receptive field properties of neurons in the feline superior colliculus

Wioletta J. Waleszczyk · Attila Nagy · Marek Wypych · Antal Berényi · Zsuzsanna Paróczy · Gabriella Eördegh · Anaida Ghazaryan · György Benedek

Received: 20 December 2005 / Accepted: 9 February 2007 / Published online: 13 March 2007

Abstract The spatio-temporal frequency response profiles of 73 neurons located in the superficial, retino-recipient layers of the feline superior colliculus (SC) were investigated. The majority of the SC cells responded optimally to very low spatial frequencies with a mean of 0.1 cycles/degree (c/deg). The spatial resolution was also low with a mean of 0.31 c/deg. The spatial frequency tuning functions were either low-pass or band-pass with a mean spatial frequency bandwidth of 1.84 octaves. The cells responded optimally to a range of temporal frequencies between 0.74 cycles/s (c/s) and 26.41 c/s with a mean of 6.84 c/s. The majority (68%) of the SC cells showed band-pass temporal frequency tuning with a mean temporal frequency bandwidth of 2.4 octaves, while smaller proportions of the SC units displayed high-pass (19%), low-pass (8%) or broad-band (5%) temporal tuning. Most of the SC units exhibited simple spectral tuning with a single maximum in the spatio-temporal frequency domain, while some neurons were tuned for spatial or temporal frequencies or speed tuned. Further, we found cells excited by gratings moving at high temporal and low spatial frequencies and cells whose activity was suppressed by high velocity movement. The spatio-temporal filter properties of the SC neurons show close similarities to those of their retinal Y and W inputs as well as those of their inputs from the cortical visual motion detector areas, suggesting their common role in motion analysis and related behavioral actions.

Keywords Spatial frequency tuning · Temporal frequency tuning · Speed tuning · Spectral receptive fields · Superior colliculus

W. J. Waleszczyk · M. Wypych · A. Ghazaryan
Department of Neurophysiology,
Nencki Institute of Experimental Biology,
3 Pasteur St., 02-093 Warsaw, Poland

A. Nagy · A. Berényi · Z. Paróczy · G. Eördegh · G. Benedek (✉)
Department of Physiology, Faculty of Medicine,
Albert Szent-Györgyi Medical and Pharmaceutical Center,
University of Szeged, Dóm tér 10, POB 427,
6720 Szeged, Hungary
e-mail: benedek@phys.szote.u-szeged.hu

Introduction

The superior colliculus (SC) is the main retino-recipient nucleus of the mammalian mesencephalon and is regarded as the homologue of the optic tectum of other vertebrate groups. It plays an important role in visually guided behavior and is involved in orienting response of the head and eyes towards the object of interest of any modality (Schneider 1969; Wurtz and Albano 1980; Stein and Meredith 1991; Schiller and Tehovnik 2001; Stein et al. 2001). In cat, as in other mammals, neurons in the superficial (retino-recipient) layers of the SC are extremely sensitive to moving stimuli (e.g. Waleszczyk et al. 1999; Dec et al. 2001; Hashemi-Nezhad et al. 2003; for earlier literature see Dreher and Hoffmann 1973; Ogasawara et al. 1984; Stein and Meredith 1991; Mendola and Payne 1993). On the basis of the velocity response profiles, neurons in the retino-recipient layers of feline SC were classified into four distinct groups (Waleszczyk et al. 1999). The neurons of three of these groups, that is, the low-velocity-excitatory (LVE), low-velocity-excitatory/high-velocity-excitatory (LVE/HVE) and high-velocity-excitatory (HVE) are regarded as saccade-related while the neurons constituting the fourth group, the low-velocity excitatory/high-velocity suppressive (LVE/HVS) are believed to participate in the fixation process.

Very few studies of the SC have focused on the spatial filter properties of the cells (Bisti and Sireteanu 1976; Pinter and Harris 1981; Mimeault et al. 2004), and to our knowledge, none of the studies yielded a detailed description of the temporal frequency characteristics of SC neurons. In the present study, therefore, we tested cat's SC neurons with sinusoidally luminance-modulated drifting gratings of a wide range of spatial and temporal frequencies and mapped out their spectral receptive fields (RFs) by plotting the responses to the gratings as functions of the spatial and temporal frequencies. Our aims were to: (1) determine the spectral RF characteristic of the feline SC neurons, and (2) to compare and update the earlier velocity response profile-based classification of the SC neurons with our new, spectral RF organization-based classification.

Preliminary results of this study have been already published (Waleszczyk et al. 2003a, b, 2004).

Materials and methods

Animal preparation

Five adult cats of either sex weighing from 2.4 to 3.5 kg were used in this study. All experimental procedures were carried out to minimize the number and the suffering of the animals and followed the European Communities Council Directive of 24 November 1986 (S6 609 EEC) and National Institutes of Health guidelines for the care and use of animals for experimental procedures. The experimental protocol had been approved by the Ethical Committee for Animal Research of Albert Szent-Györgyi Medical and Pharmaceutical Center of the University of Szeged. The animals were initially anaesthetized with ketamine hydrochloride (30 mg/kg i.m., Calypsol). To reduce salivation and bronchial secretion a subcutaneous injection of 0.2 ml 0.1% atropine sulphate was administered preoperatively. In order to minimize eye movements, bilateral cervical sympathectomy was performed (cf. Rodieck et al. 1967). The trachea and the femoral vein were cannulated and the animals were placed in a stereotaxic headholder. All wounds and pressure points were routinely infiltrated with local anesthetic (procaine hydrochloride, 1%). Throughout the surgery the anesthesia was continued with halothane (1.6%, Fluothane) in air. The animals were immobilized with initial 2 ml intravenous bolus of gallamine triethiodide (20 mg/kg). During recording sessions, liquid containing gallamine triethiodide (8 mg/kg/h), glucose (10 mg/kg/h) and dextran (50 mg/kg/h) in Ringer lactate solution was infused at a rate of 4 ml/h. Atropine sulphate (1–2 drops, 0.1%) and phenylephrine hydrochloride (1–2 drops, 10%) were applied locally to respectively dilate the pupils and block accommodation, and retract the nictitating membranes. The eye contralateral to the recording site was equipped with a +2 dioptre contact lens. The ipsilateral eye was occluded during the visual stimulation. During the recording sessions, anesthesia was maintained with a gaseous mixture of air and halothane (about 0.8%). The end-tidal concentration of halothane, MAC values and peak CO_2 concentrations were monitored with a capnometer (Capnomac Ultima, Datex-Ohmeda, Inc.). The heart rate and brain activity (electroencephalogram, EEG) were also monitored continuously. By adjustment of the concentration of halothane, the EEG maintained a slow wave record with sleep spindles. The peak expired CO_2 was kept in the range 3.7–4.3% by adjustment of the respiration rate or volume of the pulmonary pump. The body temperature was maintained at around 37°C via a warm-water heating blanket with automatic control.

A craniotomy was made above the occipital cortex overlying the SC at Horsley-Clarke co-ordinates anterior 6 to posterior 1, lateral 0 to 6. The exposed cortex was covered with 4% agar gel to prevent its dehydration.

The retinal landmarks and major retinal blood vessels were projected routinely twice daily onto a tangent screen, using a fiber optic light source (Pettigrew et al. 1979). The *area centralis* was plotted by reference to the optic disc (14.6° medially and 6.5° below the center of the optic disc; Bishop et al. 1962).

Recording, visual stimulation and data analysis

Extracellular recordings were performed from the superficial, retino-recipient layers of the SC with varnished tungsten microelectrodes (A-M Systems, Inc®, USA) with an impedance of 2–4 MΩ. The microelectrode was advanced with a microstepper. Action potentials were conventionally amplified, displayed on an oscilloscope, and transduced through a loudspeaker. Single-cell discrimination was performed with a spike-separator system (SPS-8701, Australia). The excitatory receptive field (discharge field, or "minimum response field"; Barlow et al. 1967) of an SC cell was defined as the area of visual space within which the visual stimuli elicited an increase in the firing rate of the cell. The location and the size of the discharge field were determined by using hand-operated stimuli (elongated bars or spots) that were lighter or darker than the background (cf. Barlow et al. 1967; Waleszczyk et al. 1999). Directional tuning and spatio-temporal frequency characteristic of each unit were tested with drifting sine wave gratings displayed on the monitor (refreshment rate: 60 Hz) positioned at a distance of 42.5 cm from the cat's eye. The contrast of the grating was held constant at 96% (Michelson contrast = $(L_{max} - L_{min})/(L_{max} + L_{min})$, where L_{max} and L_{min} are the maximum and minimum luminance of the spatial sinusoid, respectively). The mean luminance of the screen

was 23 cd/m^2. Stimuli were presented on the monitor within a circular aperture with a diameter of 30° centered on the center of RF of the tested cell. The presentation of the single stimulus, overall, lasted 2 s. During the first 1 s, the grating remained stationary, and it then drifted for 1 s. The interstimulus interval was 0.5 s. Neuronal activities were recorded, correlated with the stimulus presentation and stored as peristimulus time histograms (PSTHs) for further statistical analysis.

To obtain directional tuning, gratings were moved in eight different directions (0–315° at 45° increments). Each direction of a movement was presented at least 12 times, interleaved with other directions in a pseudo-random order. The preferred direction was then used for determination of the spatio-temporal frequency characteristic of the tested cell.

The spatio-temporal frequency response profiles of SC cells were assessed with the use of 24–93 spatio-temporal frequency combinations of drifting gratings. The tested spatial frequencies ranged from 0.025 to 0.95 cycles/degree (c/deg), while the temporal frequencies varied from 0.07 to 29.24 cycles/s (c/s). Stimuli were presented in pseudo-random order in series consisting of eight spatio-temporal frequency combinations of moving gratings. Each spatio-temporal frequency combination was presented at least 12 times.

The relative modulation index was calculated as the ratio of the amplitude of the response component at the fundamental (i.e. of the stimulus) temporal frequency (f_1) and the net response of the cell (f_0) (Movshon et al. 1978a). Since most of the collicular units responded to the drifting grating with an unmodulated or weakly modulated elevation of discharges, the mean discharge rate during grating movement was used as a measure of the response. Responses to grating movement were averaged over all presentations of the given spatio-temporal frequency combination. In case of the clear changes in neuronal activity during recording not related to stimulation by drifting gratings, i.e. when the mean 'spontaneous' (background) activity of the cell for any series varied more than two SEM from the 'spontaneous' activity measured for any other series, the cell was excluded from later analysis.

The spatio-temporal frequency RFs (spectral RFs) were constructed from the recorded responses (e.g. Fig. 1) through the use of surface fitting (MATLAB® software, MathWorks, Inc.). For most of the cells, the response to spatial frequency depended on the temporal frequency of the drifting grating. Thus, assessment of the spatial frequency tuning with a fixed temporal frequency of grating or of the temporal frequency tuning with a fixed spatial frequency of drifting grating would have resulted in an underestimation of the spatial or temporal bandwidth, respectively. Accordingly, spatial and temporal frequency tuning curves were derived from the two-dimensional spatio-temporal frequency response profiles of the cell by fitting the curve to data-points located in the region of peak sensitivity, using triangle-based cubic interpolation (MATLAB®), a procedure, which corresponds roughly to transection of the spectral RF by a plane oriented along or orthogonal to the optimum spatio-temporal frequency combinations of grating. Optimum orientation of the transection plane was obtained by means of Principal Component Analysis (PCA, Harman 1976). PCA is a linear transformation of multidimensional data into new orthogonal coordinate system, such that the direction of greatest variance of data defines first coordinate (i.e. most meaningful underlying variable, called first principal component). Consecutive components indicate directions (variables) explaining most of remaining variance of data. After transformation, all data can be described as linear combination of new variables (principal components). Here we used this method to find the orientation of area of response in the two-dimensional spatio-temporal frequency response profile of the cell and to derive spatial and temporal frequency tuning curves (e.g. Figs. 2, 5, 6). PCA was applied (in MATLAB®) to the set of points, in which interpolated cell responses exceeded a given threshold (0.5 of the maximum response). The orientation of the transection plane corresponded to the main or orthogonal direction found by PCA, with the additional condition that the plane had to contain the maximum response point (see the example in Fig. 2). The spatial or temporal frequency tuning curve was obtained for the direction which corresponded to the grater variance of the data in spatial or temporal frequencies, respectively.

The spatial or temporal frequency bandwidth was measured as the full width at half-height of the spatial or temporal frequency tuning curve of the cell. The spatial high-frequency cut-off, regarded as a measure of spatial resolution (acuity), was defined as the frequency at which the response of the cell (after subtraction of 'spontaneous' activity) fell to one-tenth of the maximum (Campbell et al. 1969; Saul and Humphrey 1990).

Localization of recording sites

At the end of the recording session, the animals were deeply anaesthetized with an intravenous injection of 160 mg of sodium pentobarbitone (Nembutal) and perfused transcardially with 500 ml of warm (37°C) saline followed by 1,000 ml of a 4% solution of paraformaldehyde in 0.1 M phosphate buffer (pH 7.4). The brains were sectioned coronally at 50 μm on a freezing microtome, mounted on gelatinized slides, and counterstained with cresyl violet. Recording sites were localized based on marks of electrode penetrations and/or electrolytic lesions.

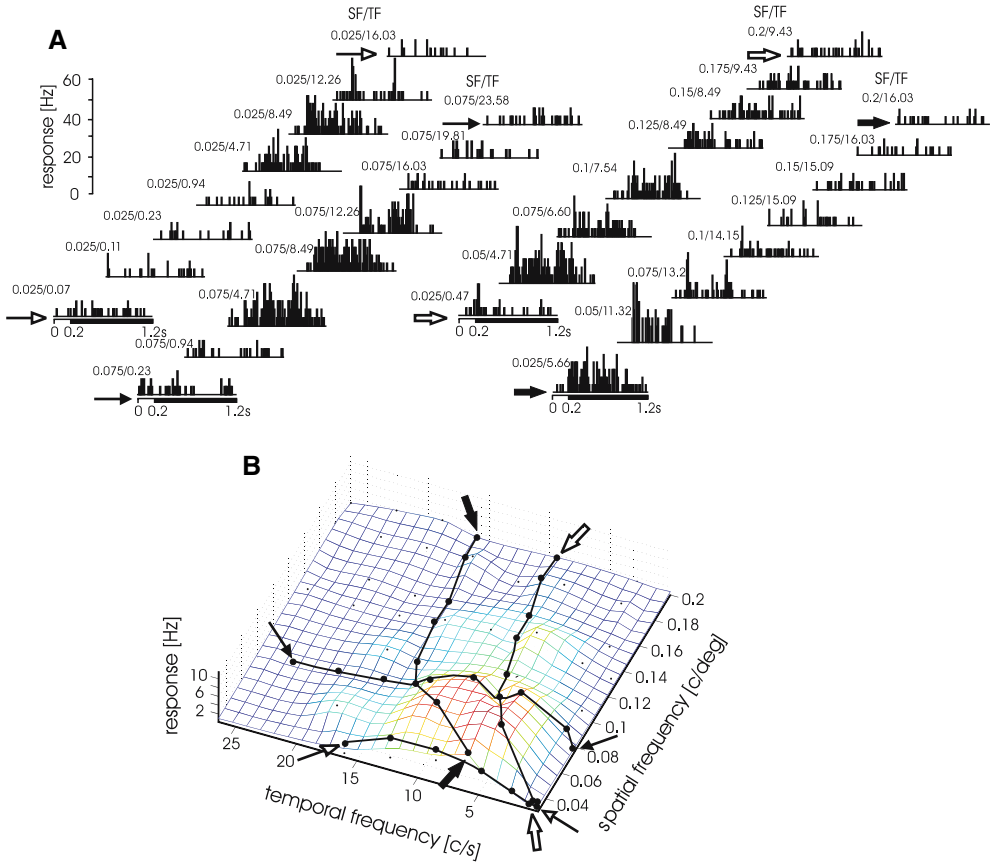

Fig. 1 Construction of the spectral receptive fields (RFs). **A** Peristimulus time histograms (PSTHs) depicting the responses of one superior colliculus (SC) unit to sinusoidal gratings drifting in the preferred direction at various spatial and temporal frequency combinations. The actual spatial and temporal frequency values of the stimulus are given on the *left side* of each PSTH in cycles per degree (c/deg)/cycles per second (c/s). The *thick lines* below the *lowermost* histograms indicate the movement of the stimulus for 1 s. The bin width was 20 ms. The four pairs of differently shaped *horizontal arrows* on the *left* of the *lowermost* and *uppermost* histograms refer to the four individual lines of the mesh plot given in part **B**. Abbreviations: *SF* spatial frequency, *TF* temporal frequency. **B** *Top view* of the perspective mesh plot of the spectral RF of this unit. The surface of the mesh was constructed by fitting to the responses (some of which shown in part **A**) to drifting gratings of different spatial and temporal frequencies. The response intensities denoted by *black dots* are the values of the mean discharge rate in Hz. The *lines* indicated at their ends by the four types of *arrows* are constructed from the corresponding PSTHs presented in part **A**

Statistical analysis of the data

All averaged data are presented as means with the standard error (SEM). Statistical analysis was performed with the SPSS® for Windows software (SPSS Inc.).

Results

Altogether, the responses of 77 SC neurons to drifting sinusoidal gratings were recorded. Of these, in 73 cells we have analyzed in detail their spatial and temporal frequency response properties. All neurons were located in the superficial, retino-recipient layers of the SC and the centers of their RFs were located within 26° from the *area centralis*. The responses to drifting gratings were usually characterized by weakly modulated or unmodulated increase in cell's discharge rate, however, the activity of some neurons was suppressed for some spatio-temporal frequency combinations and/or the directions of moving gratings.

The relative modulation index of responses to gratings moving at optimum spatial and temporal frequencies (at peak f_0) was calculated for 59 neurons. The mean relative modulation index for these cells was 0.49 ± 0.03 (range 0.18–1.32).

Spatial frequency characteristics of SC neurons

Like the cell whose responses are illustrated in Fig. 2 (Fig. 2A–C), most cells responded optimally to very low spatial frequencies (Fig. 3A). The mean optimal spatial frequency for the whole sample was 0.10 ± 0.01 c/deg (range

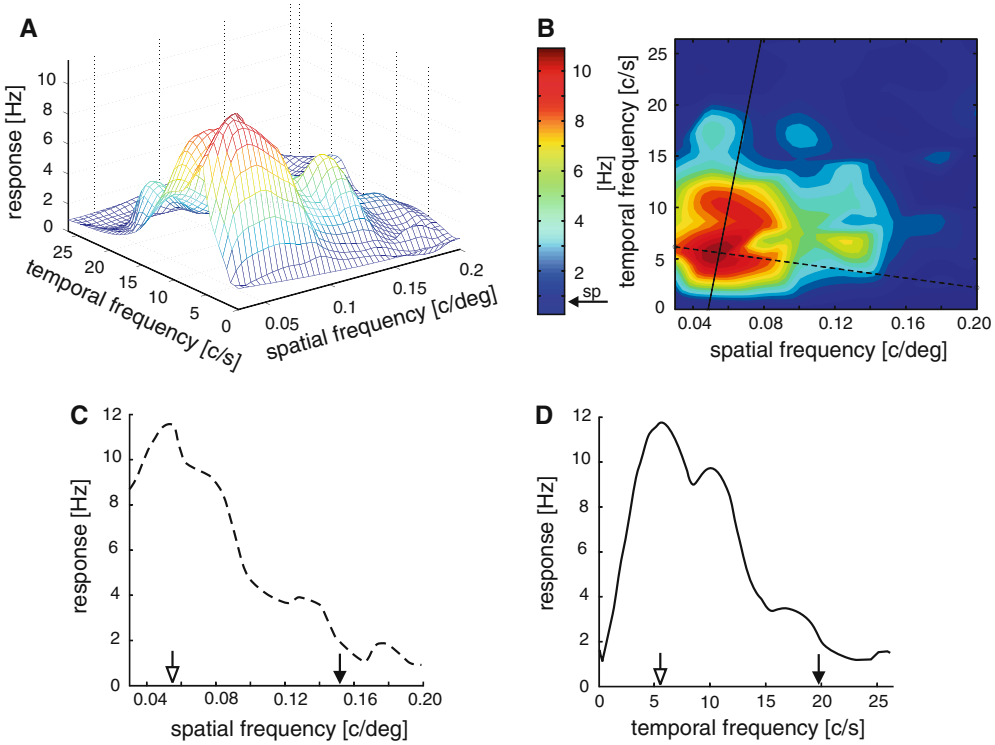

Fig. 2 Spatio-temporal frequency response profile of the SC cell with simple tuning. **A** Perspective mesh plot of the spectral RF of the cell, whose responses are shown in Fig. 1**A**. Intensity of the responses is coded in color. A *colored scale bar* is shown on the *right*. The *arrow* with "*sp*" label indicates the level of 'spontaneous' activity. **B** Contour plot of the spectral RF. The *solid line* denotes the main direction assigned by principal component analysis (PCA). The *dashed line* indicates values orthogonal to the main direction. The intersection point of the two lines indicates the maximum response and optimum spatial and temporal frequencies. **C** Spatial frequency tuning curve obtained by transection through the spectral RF along the orthogonal to the main PCA direction represented by a *dashed line* in **B**. **D** Temporal frequency tuning curve obtained by the transection through the spectral receptive field along the main PCA direction represented by *solid line* in **B**. Open *arrows* in **C** and **D** indicate optimum spatial and temporal frequencies, respectively. *Filled arrows* indicate the spatial and temporal resolution (one tenth of the maximal response)

0.03–0.47 c/deg). Furthermore, since for a substantial proportion of cells (12/72; 17%) the optimal spatial frequency was at the lowest frequency tested, the mean optimal frequency could be an overestimate.

Just over a half (37/72; 51%) of the cells in our sample displayed spatial low-pass tuning and there was either no or only a slight attenuation of the response at low spatial frequencies. The tuning curve of SC neuron presented in Fig. 2C displays spatial low-pass characteristics with a typical optimum at low spatial frequencies. The remainder of the units (35/72; 49%) exhibited band-pass spatial frequency tuning. In these cells, there was an attenuation of the response to at least half the height of the maximum. For cells with spatial band-pass characteristics, the mean spatial frequency bandwidth was 1.84 ± 0.15 octaves (range 0.39–3.60 octaves; Fig. 3B).

The distribution of the spatial resolutions for the sample of 68 SC cells is presented in Fig. 3c. Two units had the high-frequency cut-off above the highest tested spatial frequency (>0.95 c/deg). The spatial resolution of the remaining cells ranged between 0.04 and 0.95 c/deg with a mean of 0.31 ± 0.03 c/deg.

Temporal frequency characteristics of SC neurons

The majority of collicular neurons (42/62; 68%) were classified as temporal band-pass cells (Fig. 4A, examples in Figs. 2D, 5Cd). About a fifth (12/62; 19%) of the sample was classified as temporal high-pass cells (an example in Fig. 6Ad), while almost one tenth (5/62; 8%) of the sample was classified as temporal low-pass cells (an example in Fig. 5Ad). The remaining 5% (3/62) of the cells were classified as temporal broad-band cells (an example in Fig. 5Bd). The mean temporal frequency bandwidth was 2.38 ± 0.22 octaves (range 0.40–5.90 octaves: Fig. 4B).

The distribution of optimum temporal frequencies in our sample is presented in Fig. 4C. The lowest optimal temporal frequency found was 0.74 c/s. For five temporal high-pass cells; the maximum response was obtained at the highest temporal frequency tested at the optimum spatial frequency (16.03 c/s for three cells, 21.69 c/s for one cell and 26.41 c/s for another cell). Including these temporal high-pass cells the mean optimal temporal frequency was 6.84 ± 0.71 c/s. Since the optimal temporal frequency could be higher than the highest temporal frequency for five cells

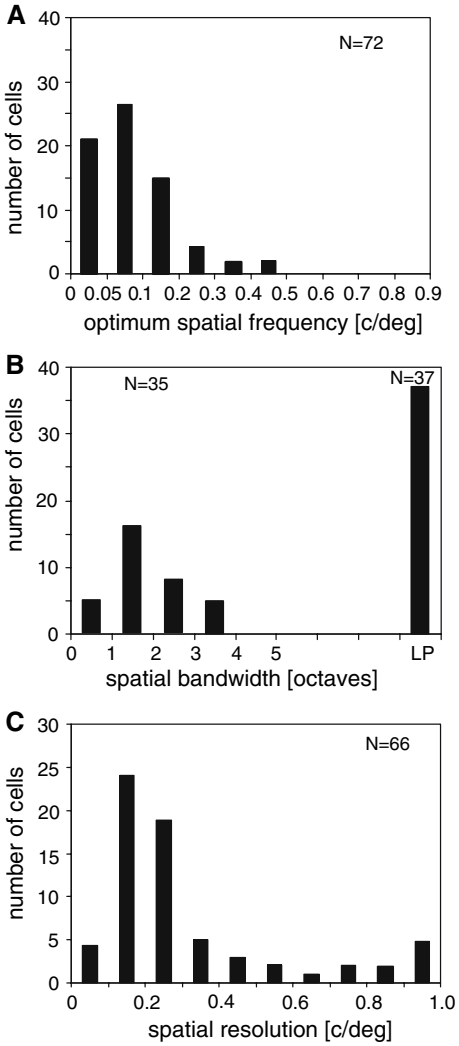

Fig. 3 Spatial frequency tuning characteristics of SC neurons. **A** Distribution of the optimum spatial frequencies in the 72 collicular neurons studied. **B** Distribution of the spatial frequency bandwidths calculated from the spatial frequency tuning curves of band-pass SC neurons ($N = 35$). *LP* indicates low-pass SC cells ($N = 37$). **C** Distribution of the spatial resolution in 66 neurons. The abscissa denotes the spatial resolution calculated from the spatial frequency tuning curves

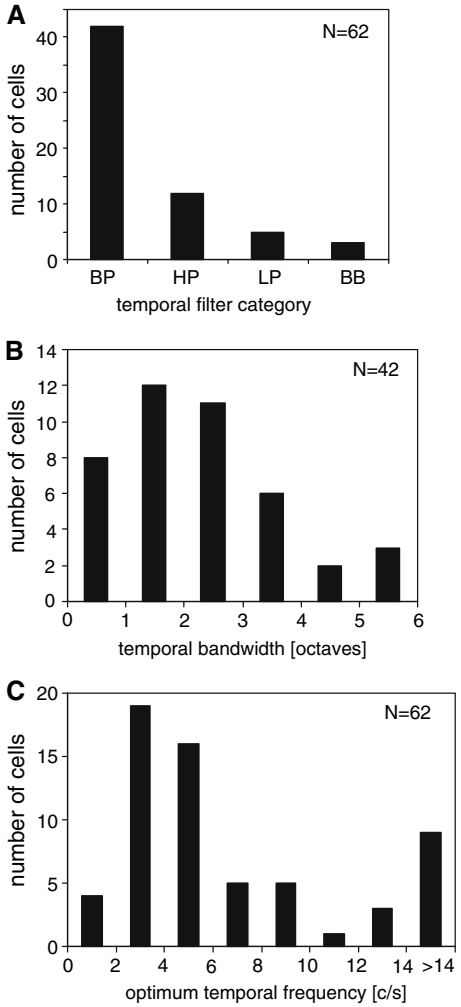

Fig. 4 Temporal frequency tuning characteristics of SC neurons. **A** Frequency distribution of 62 SC cells in each temporal filter category (*BP* band-pass, *HP* high-pass, *LP* low-pass and *BB* broad-band category). **B** Distribution of 42 band-pass SC cells according to their temporal frequency bandwidths calculated in octaves. **C** Distribution of 62 collicular cells according to their optimum temporal frequencies

tested, the above mean temporal frequency value could be an underestimate.

Spectral receptive fields in the SC

The spatio-temporal frequency respective fields were obtained for 59 SC cells for responses to the sinusoidal gratings drifting in the optimal direction. Almost half of the cells (29/59, 49%) exhibited a spatio-temporal frequency response profile characterized by a region of increased activity with a single maximum in the spatio-temporal frequency domain (simple tuning). The spectral RF of such neuron is exemplified in Fig. 2. In Fig. 1A, the responses of this cell to drifting sinusoidal gratings are presented in the form of PSTHs. The profile of the spectral RF indicates the existence of a single oval region of increased activity (Fig. 2A, B). Note, that the spatial frequency tuning curve with a maximum at 0.05 c/deg does not fall below the half-amplitude on the side of low spatial frequencies (Fig. 2C), and thus the cell was classified as a low-pass one. The temporal frequency tuning curve of this neuron (Fig. 2D) was characteristic for band-pass cells. Mean optimum velocity of moving gratings (optimal temporal frequency/optimal spatial frequency) for neurons showing simple tuning was 85.9 ± 13.2 deg/s (range 10.8–364.5 deg/s). Neurons constituting this group were recorded in upper and lower part of the *stratum griseum superficiale* (SGSu and SGSl), and *stratum opticum* (SO).

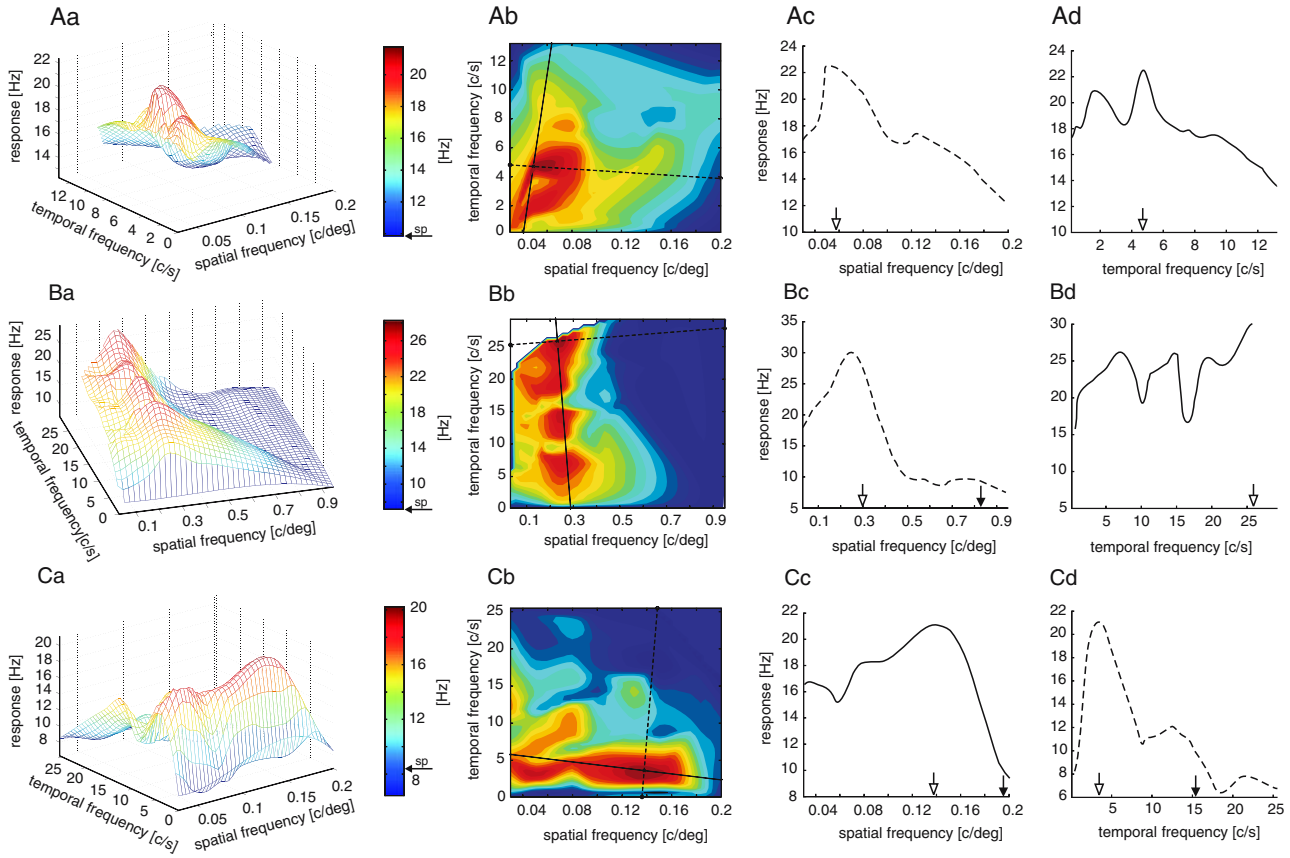

Fig. 5 Typical examples of different spectral receptive fields of SC cells. **A** Example of the spectral receptive field of speed-tuned SC neuron. *Aa*, *Ab*. Perspective and contour plots, respectively of the spectral RF of a speed-tuned cell. The response profile reveals relatively narrow speed tuning. *Ac*, *Ad*. Spatial and temporal frequency tuning curves obtained by transection through the spectral RF along the orthogonal and main PCA directions (the *dashed* and *solid lines*, respectively, in *Ab*). **B** Example of spectral RFs of SC cells showing spatial tuning. *Ba*, *Bb*. Perspective and contour plots of the spectral RF field showing spatial tuning. The region of peak sensitivity is parallel to the temporal frequency axis. *Bc*, *Bd*. Spatial and temporal frequency *tuning curves* obtained by the transection through the spectral RF along the orthogonal and main the PCA directions (the *dashed* and *solid* lines, respectively, in *Bb*). Note the relatively broad temporal tuning. **C** Example of spectral RFs of SC cells showing temporal tuning. *Ca*, *Cb*. Perspective and contour plots of the spectral RF showing temporal tuning. The region of peak sensitivity is parallel to the spatial frequency axis. *Cc*, *Cd*. Spatial and temporal frequency tuning curves obtained by transection through the spectral RF along the main and orthogonal PCA directions (the *solid* and *dashed* lines, respectively, in *Cb*). Note the relatively broad spatial and narrow temporal tuning. Other conventions the same as in Fig. 2

In over a third of the sample (22/59; 37%), the region of increased activity was elongated, forming a ridge of peak sensitivity parallel to the temporal or the spatial frequency axis or oriented relative to the axes indicating spatial, temporal or speed tuning, respectively (for a classification see Clifford and Ibbotson 2003). Eleven of the 59 SC units (18.5%) were speed-tuned, while six (10%) displayed spatial frequency tuning and five (8.5%) temporal frequency tuning.

Figures 5Aa and b show the spectral RF of a neuron for which the response to spatial frequencies varied with the temporal frequency of the stimulus, forming an elongated ridge of peak sensitivity oriented relative to the spatial and temporal frequency axes, indicating speed tuning. The spatial and temporal frequency tuning curves (Fig. 5Ac, d, respectively) indicate low-pass characteristic in both the spatial and temporal frequency domains. Mean optimum velocity of moving gratings for neurons in the group showing speed tuning was 83.0 ± 10.5 deg/s (range 33.3–131.7 deg/s). The neurons were located in all retino-recipient layers of the SC (SGSu, SGSl, SO and the upper part of the *stratum griseum intermediale*; SGIu).

In Fig. 5B, the spectral RF of the cell which was sensitive to a particular spatial frequency is presented. The response profile of this neuron displays an elongated ridge over a wide range of temporal frequencies in the limited range of spatial frequencies (spatial tuning). The cell was classified as broad-band in the temporal frequency domain (Fig. 5Bd). The typical features of cells which show spatial tuning were a relatively high optimum spatial frequency (mean 0.29 c/deg vs. 0.1 c/deg for the whole sample) and spatial resolution (mean 0.76 c/deg vs. 0.31 c/deg for the whole sample; e.g. Fig. 5Bc). Mean optimum velocity of

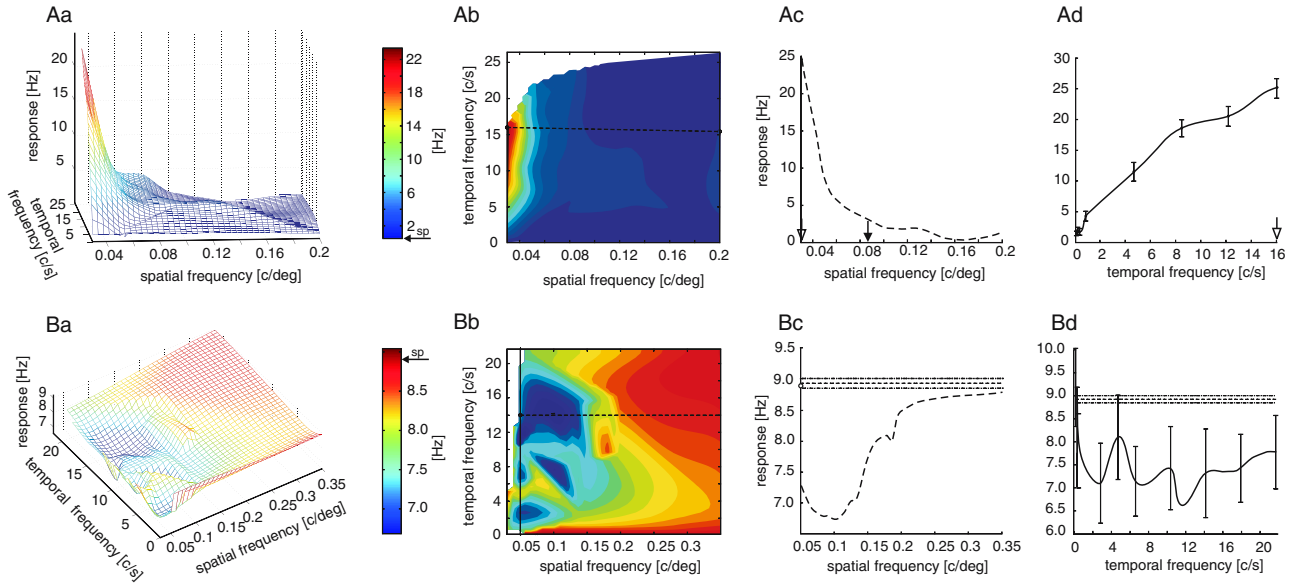

Fig. 6 Further examples of spectral RFs of SC cells. **A** Example of a spectral receptive field (*Aa*, *b*) of a cell whose location of peak sensitivity indicates good responsiveness to high velocities and/or fast changes of large images. The cell was characterized by low-pass spatial frequency (*Ac*) and high-pass temporal frequency properties (*Ad*). The cell was not sensitive for a direction of grating movement and spatio-temporal frequency response profile obtained for the opposite direction of the stimulus movement was very similar. **B** Example of a spectral receptive field (*Ba*, *b*) of a cell showing suppression of activity in the region of the spatial and temporal frequencies corresponding to high speed of the moving stimulus. Suppression was also observed for other directions of grating movement. Spatial frequency tuning curves in *Ac* and *Bc* were obtained for transections through spectral receptive fields parallel to spatial frequency axis (*dashed lines*) at 16 and 14 Hz, respectively. Temporal frequency tuning curves were plotted on the basis of recorded responses at the spatial frequency of 0.025 cycles/deg in *Ad* and 0.05 cycles/deg in *Bd*. Points are the means of the measured responses (±SEM). The *thin dashed lines* in *Bc* and *Bd* denote the level of spontaneous activity (±SEM). Other conventions are the same as in Fig. 2

moving gratings for neurons in this group was 27.8 ± 10.9 deg/s (range 12.4–74.5 deg/s). Such neurons were recorded in SGSu and SGSl.

A typical spectral receptive field of the cells which displayed temporal tuning with response profile elongated parallel to the spatial frequency axis is shown in Fig. 5Ca and b. The cell exhibited relatively broad tuning in the spatial frequency domain (Fig. 5Cc), and narrow tuning in the temporal frequency domain (Fig. 5Cd). Mean optimum velocity of moving gratings for neurons showing temporal tuning was 35.4 ± 6.8 deg/s (range 22.4–55.0 deg/s). These neurons were recorded from SGSu and SGSl.

Figure 6Aa illustrates the spectral spatio-temporal response profile of the cell which was sensitive to very low spatial frequencies and responded vigorously to a grating moving with relatively high velocity. All cells in this group (6 of the 59 SC cells, 10%) could be classified as low-pass ones in the spatial frequency domain and high-pass ones in the temporal frequency domain (e.g. Fig. 6Ac and Ad). In the temporal domain, a small attenuation of the response was observed at the high temporal frequencies tested for some cells, but in no case did the decrease reach the half of the maximum response. Mean optimum velocity of moving gratings for neurons in this group was 333.8 ± 57.5 deg/s (range 155.0–509.7 deg/s). These values are underestimated because of spatial frequency low-pass and temporal frequency high-pass characteristics of cells. These neurons were recorded from SGS.

A small population of the SC cells (2 out of 59; 3.5%) exhibited suppression in the spatio-temporal frequency plain corresponding to a high velocity of grating movement. In Fig. 6B, the characteristics of one of these spectral RFs is presented. Only one neuron showed clear excitation in spatio-temporal frequency response profile and the optimum velocity of moving gratings for this neuron was 37.4 deg/s. Neurons showing suppression in the spectral RF profiles were found in SO in the rostral part of the SC. Centers of the RFs of these neurons were located close to *area centrales*.

In the penetrations through the superficial layers of the SC we found several remarkable clustering of neurons with similar spectral characteristics. The relatively low number of neurons analyzed, however, prevented us from drawing conclusions concerning clustering of cells of certain types in separate layers of the SC.

Discussion

Despite the large number of electrophysiological studies on the SC, very little information is available on the spectral

RF properties of the neurons in this structure. We report here on a detailed spatio-temporal frequency response profiles of the SC units, describing simple, spatial and temporal tuned neurons in the SC and providing the first evidence on speed-tuned cells in the tectal region of the mammalian brain.

Consistent with earlier reports (Pinter and Harris 1981; Mimeault et al. 2004), the majority of the SC cells in our study responded optimally to very low spatial frequencies with a mean of 0.10 c/deg. This indicates that cells in the SC act as good low-pass filters in the spatial frequency domain. The low optimal spatial frequency and the low spatial resolution of the SC neurons (mean of 0.31 c/deg) is not surprising taking into account that the retinal input to the SC is restricted to W and Y retinal ganglion cells (for a review see Waleszczyk et al. 2004; cf. Rowe and Cox 1993). Similarly, low optimal spatial frequency and low spatial resolution were reported in the literature for the W- and Y-type cells in the cat dorsal lateral geniculate nucleus (LGNd) (Sireteanu and Hoffmann 1979; Sur and Sherman 1982; Saul and Humphrey 1990), cells in cortical areas of the cat dominated by the W-input, e.g. area 19 (Tardif et al. 1997; Bergeron et al. 1998) or belonging to the motion- rather than pattern-processing stream dominated by the Y-input, e.g. area 18 (Movshon et al. 1978b; Berardi et al. 1982), the lateral suprasylvian cortices: the posteromedial lateral suprasylvian area (PMLS) (Di Stefano et al. 1985; Zumbroich and Blakemore 1987; Minville and Casanova 1998; Merabet et al. 2000), the posterolateral lateral suprasylvian area (PLLS) (Zumbroich and Blakemore 1987), the anteromedial lateral suprasylvian area (AMLS) (Ouellette et al. 2004), the anterior ectosylvian visual area (AEV) (Nagy et al. 2003) and cells in area 21b (Tardif et al. 2000). On the other hand, the mean optimal spatial frequency and spatial resolution of our sample of SC neurons are much lower than these of LGNd X-type cells (Saul and Humphrey 1990; Sireteanu and Hoffmann 1979) and these of neurons in area 17 dominated by X input (Maffei and Fiorentini 1973; Eggers and Blakemore 1978; Movshon et al. 1978b) or even these of population cortico-tectal cells in area 17 (Casanova 1993) and also lower than that of cells in area 21a (Tardif et al. 1996; Morley and Vickery 1997), an another cortical area dominated by X input which belongs to the 'form' pathway (Dreher et al. 1993; Burke et al. 1998).

Our results indicate that the SC neurons respond to a wide range of temporal frequencies. We have found cells with maximum responses at a temporal frequency as low as 0.74 c/s and as high as 26.4 c/s. The mean optimal temporal frequency of collicular cells recorded in the present study (6.8 c/s) is in line with earlier findings (Pinter and Harris 1981) and is comparable to the mean values for the AEV (6.3 c/s; Nagy et al. 2003), the PMLS (range 2–10 c/s; Morrone et al. 1986; Zumbroich and Blakemore 1987), and the AMLS area (4.5 c/s; Ouellette et al. 2004), while it is higher than the mean value for other visual cortical areas (Saul and Humphrey 1992; Casanova 1993; Morley and Vickery 1997; Bergeron et al. 1998; Tardif et al. 2000; see however Tardif et al. 1996). Preference for high temporal frequencies of some cells in the SC, like those in the AEV, PMLS, PLLS and AMLS areas most likely reflects the predominance of Y-type input to these brain regions. Surprisingly, area 18 that is dominated by Y-type input has relatively low mean optimal temporal frequency (3.2 c/s; Saul and Humphrey 1992). Thus, the SC seems to be an important source of visual information in the high temporal frequencies relayed via extrageniculate visual thalamus to cortical neurons in the lateral suprasylvian and in the anterior ectosylvian cortices, areas which participate in motion analysis (Hicks et al. 1986; Norita et al. 1986, 1996; Olson and Graybiel 1987; Abramson and Chalupa 1988; Katoh and Benedek 1995; Nagy et al. 2003).

With regard to the spatio-temporal frequency response profiles observed, we can classify the SC units into the following six groups:

Group 1 Almost a half of the investigated SC units displayed simple spatio-temporal tuning, characterized by a region of increased activity with a single maximum in the spatio-temporal frequency domain. These neurons responded in a broad range of velocities with a preference for velocity determined by optimum spatial and temporal frequency.

Group 2 About 20% of the SC neurons in our sample demonstrated spectral RFs forming an elongated ridge of peak sensitivity oriented relative to the spatial and temporal frequency axes. This indicates that these neurons responded selectively to a set of particular spatio-temporal frequency combinations, i.e. to a certain speed of stimulus movement. Speed-tuned cells have not been reported earlier in the mammalian SC; they have been found so far in area 17 and in the middle temporal cortical visual motion area (MT area) of macaque monkey (Newsome et al. 1983; Perrone and Thiele 2001, 2002; Priebe et al. 2003; Priebe et al. 2006), in area 18 of the cat (Friend and Baker 1993), in the pretectal nucleus of the optic tract (NOT) of the tammar wallaby (Ibbotson and Price 2001), in the nucleus *lentiformis mesencephali*, an avian homologue of the mammalian NOT (Wylie and Crowder 2000; Ibbotson and Price 2001) and also in the avian nucleus of the basal optic root of the accessory optic system (Crowder et al. 2003). By examining the responses of the neurons in spatio-temporal frequency space, Perrone and Thiele (2001) confirmed that these neurons have properties that are closely matched to the most commonly used stimulus, i.e. moving bars.

Groups 3 and *4* The next two groups of SC neurons had spectral RFs which displayed spatial or temporal frequency

tuning. Spatial frequency tuning is a characteristic feature of neurons in feline primary visual cortex: in area 17 (Tolhurst and Movshon 1975; Bisti et al. 1985; Friend and Baker 1993) and in area 18 (Friend and Baker 1993). Here the optimal spatial frequency is invariant with respect to the temporal frequency. The relatively high values of optimum spatial frequency and spatial resolution in the group of SC cells showing spatial frequency tuning indicate that spectral RF properties of these neurons may be determined by the input from primary visual cortex. Indeed, optimum spatial frequency and spatial resolution of area 17 cortico-tectal cells (mean 0.7 c/deg and 1.8 c/deg, respectively; Casanova 1993) are much higher than means for the whole sample of SC cells. The spatio-temporal frequency response characteristics of the above-described four groups of SC neurons indicate that these cells could correspond to LVE or LVE/HVE cells distinguished on the basis of the velocity response profiles (Waleszczyk et al. 1999).

Group 5 About 10% of the SC cells in our sample had RF profiles showing maximum sensitivity at very low spatial frequencies and relatively high temporal frequencies. Cells with such spectral RFs could correspond to SC HVE cells (Waleszczyk et al. 1999). However, the profile of spectral receptive field characterized by maximum sensitivity at high temporal frequencies and very low spatial frequencies (Fig. 6A) indicates that these neurons do not act as high velocity detectors but rather code motion-related changes in contrast and luminance which may occur during saccade-like displacement of the visual field, like it was suggested for, having similar spatio-temporal frequency response profile, non-directional neurons in pretectum (NOT) of wallaby and pigeon *nucleus lentiformis mesencephali* (fast cells; Ibbotson et al. 1994; Ibbotson and Mark 1994; Ibbotson and Price 2001; cf. jerk cells; Schoppmann and Hoffmann 1979; Hoffmann and Distler 1989).

Group 6 of SC cells demonstrated suppression at low spatial frequencies and high velocities of moving gratings. Cells with similar spatio-temporal frequency characteristics have been found also in the NOT and the dorsal terminal nucleus of the accessory optic system of the marsupial tammar wallaby (Ibbotson et al. 1994). Collicular cells with such a response profile could correspond to low-velocity-excitatory and high-velocity-suppressive (LVE/HVS) cells reported earlier (Waleszczyk et al. 1999). As in the case of LVE/HVS cells the activity of these units was suppressed by fast movement of visual stimulus in any direction (cf. Waleszczyk et al. 1999). These cells most likely correspond to "fixation" cells, a group of premotor neurons found in the rostral part of the SC during recordings in behaving cats and macaques (Guitton and Munoz 1991; Munoz and Guitton 1991; Munoz and Wurtz 1993a, b; Peck and Baro 1997; Bergeron and Guitton 2001; Lünenburger et al. 2001).

The spatio-temporal characteristics found in the SC are in line with the notion that the SC is involved in orienting behavior (Schneider 1969; Sprague 1996). The relatively broad spatial and temporal frequency tuning found in the SC accords with the neuronal requirements of this behavior. The robust responsiveness of SC cells to a broad range of temporal frequencies increases the chance of stimulus detection, regardless of its properties. Such a function can be deduced from other properties of SC cells, such as the relatively large size of the RFs, reflecting the multiple inputs from spatially non-overlapping RFs or the broad range of velocity responses as a consequence of the convergence of Y- and W-type inputs (Waleszczyk et al. 1999; Wang et al. 2001). The preference for low spatial frequencies combined with a large range of temporal frequencies indicates that a population of SC cells would respond well to large objects moving at a wide range of velocities. SC neurons with spectral RFs showing speed tuning are most probably involved in the detection of objects moving with a particular velocity, while the other SC neurons are most likely involved in detection of stimuli in a broad range of velocities. Thus, the wide varieties of spatio-temporal frequency response profiles may represent different functional neuronal groups within the SC that sub-serve different behavioral actions needed to meet various environmental requirements.

Acknowledgments We thank Zita Márkus and Alice Roxin, medical students at Albert Szent-Györgyi Medical and Pharmaceutical Center, for their participation in some of the experiments described here, Gabriella Dósai for her skilful technical assistance, and Péter Liszli for computer programming. Thanks are due to Prof. Bogdan Dreher and the reviewers for their helpful comments on the manuscript. The work was supported financially by the Polish State Committee for Scientific Research grant no. 3P04C08222, Hungarian OTKA grant no. T042610 and ETT grant no. 429/2003.

References

Abramson BP, Chalupa LM (1988) Multiple pathways from the superior colliculus to the extrageniculate visual thalamus of the cat. J Comp Neurol 271:397–418

Barlow HB, Blakemore C, Pettigrew JD (1967) The neural mechanism of binocular depth discrimination. J Physiol (Lond) 193:327–342

Berardi N, Bisti S, Cattaneo A, Fiorentini A, Maffei L (1982) Correlation between the preferred orientation and spatial frequency of neurones in visual areas 17 and 18 of the cat. J Physiol (Lond) 323:603–618

Bergeron A, Guitton D (2001) The superior colliculus and its control of fixation behavior via projections to brainstem omnipause neurons. Prog Brain Res 134:97–107

Bergeron A, Tardif E, Lepore F, Guillemot JP (1998) Spatial and temporal matching of receptive field properties of binocular cells in area 19 of the cat. Neuroscience 86:121–134

Bishop PO, Kozak W, Vakkur GJ (1962) Some quantitative aspects of the cat's eye: axis and plane of reference, visual field coordinates and optics. J Physiol (Lond) 163:466–502

Bisti S, Sireteanu RC (1976) Sensitivity to spatial frequency and contrast of visual cells in the cat superior colliculus. Vision Res 16:247–251
Bisti S, Carmignoto G, Galli L, Maffei L (1985) Spatial-frequency characteristics of neurones of area 18 in the cat: dependence on the velocity of the visual stimulus. J Physiol (Lond) 359:259–268
Burke W, Dreher B, Wang C (1998) Selective block of conduction in Y optic nerve fibres: significance for the concept of parallel processing. Eur J Neurosci 10:8–19
Campbell FW, Cooper GF, Enroth-Cugell C (1969) The spatial selectivity of the visual cells of the cat. J Physiol (Lond) 203:223–235
Casanova C (1993) Response properties of neurons in area 17 projecting to the striate-recipient zone of the cat's lateralis posterior-pulvinar complex: comparison with cortico-tectal cells. Exp Brain Res 96:247–259
Clifford CW, Ibbotson MR (2003) Fundamental mechanisms of visual motion detection: models, cells and functions. Prog Neurobiol 68: 409–437
Crowder NA, Dawson MR, Wylie DR (2003) Temporal frequency and velocity-like tuning in the pigeon accessory optic system. J Neurophysiol 90:1829–1841
Dec K, Waleszczyk WJ, Wróbel A, Harutiunian-Kozak BA (2001) The spatial substructure of visual receptive fields in the cat's superior colliculus. Arch Ital Biol 139:337–355
Di Stefano M, Morrone MC, Burr DC (1985) Visual acuity of neurones in the cat lateral suprasylvian cortex. Brain Res 331:382–385
Dreher B, Hoffmann KP (1973) Properties of excitatory and inhibitory regions in the receptive fields of single units in the cat's superior colliculus. Exp Brain Res 16:333–353
Dreher B, Michalski A, Ho RH, Lee CW, Burke W (1993) Processing form and motion in area 21a of cat visual cortex. Vis Neurosci 10:93–115
Eggers HM, Blakemore C (1978) Physiological basis of anisometropic amblyopia. Science 201:264–267
Friend SM, Baker CL Jr (1993) Spatio-temporal frequency separability in area 18 neurons of the cat. Vision Res 33:1765–1771
Guitton D, Munoz DP (1991) Control of orienting gaze shifts by the tectoreticulospinal system in the head-free cat. I. Identification, localization, and effects of behavior on sensory responses. J Neurophysiol 66:1605–1623
Harman HH (1976) Modern factor analysis (revised), 3rd edn. University of Chicago Press, Chicago
Hashemi-Nezhad M, Wang C, Burke W, Dreher B (2003) Area 21a of cat visual cortex strongly modulates neuronal activities in the superior colliculus. J Physiol (Lond) 550:535–552
Hicks TP, Stark CA, Fletcher WA (1986) Origins of afferents to visual suprageniculate nucleus of the cat. J Comp Neurol 246:544–554
Hoffmann KP, Dreher B (1973) The spatial organisation of the excitatory region of receptive fields in the cat's superior colliculus. Exp Brain Res 16:354–370
Hoffmann KP, Distler C (1989) Quantitative analysis of visual receptive fields of neurons in nucleus of the optic tract and dorsal terminal nucleus of the accessory optic tract in macaque monkey. J Neurophysiol 62:416–428
Ibbotson MR, Mark RF (1994) Wide-field nondirectional visual units in the pretectum: do they suppress ocular following of saccade-induced visual stimulation. J Neurophysiol 72:1448–1450
Ibbotson MR, Price NSC (2001) Spatiotemporal tuning of directional neurons in mammalian and avian pretectum: a comparison of physiological properties. J Neurophysiol 86:2621–2624
Ibbotson MR, Mark RF, Maddess TL (1994) Spatiotemporal response properties of direction-selective neurons in the nucleus of the optic tract and dorsal terminal nucleus of the wallaby, *Macropus eugenii*. J Neurophysiol 72:2927–2943
Katoh YY, Benedek G (1995) Organization of the colliculo-suprageniculate pathway in the cat: a wheat germ agglutinin-horseradish peroxidase study. J Comp Neurol 352:381–397
Lünenburger L, Kleiser R, Stuphorn V, Miller LE, Hoffmann KP (2001) A possible role of the superior colliculus in eye-hand coordination. Prog Brain Res 134:109–125
Maffei L, Fiorentini A (1973) The visual cortex as a spatial frequency analyser. Vision Res 13:1255–1267
Mendola JD, Payne BR (1993) Direction selectivity and physiological compensation in the superior colliculus following removal of areas 17 and 18. Vis Neurosci 10:1019–1026
Merabet L, Minville K, Ptito M, Casanova C (2000) Responses of neurons in the cat posteromedial lateral suprasylvian cortex to moving texture patterns. Neuroscience 97:611–623
Mimeault D, Paquet V, Molotchnikoff S, Lepore F, Guillemot JP (2004) Disparity sensitivity in the superior colliculus of the cat. Brain Res 1010:87–94
Minville K, Casanova C (1998) Spatial frequency processing in posteromedial lateral suprasylvian cortex does not depend on the projections from the striate-recipient zone of the cat's lateral posterior-pulvinar complex. Neuroscience 84:699–711
Morley JW, Vickery RM (1997) Spatial and temporal frequency selectivity of cells in area 21a of the cat. J Physiol (Lond) 501:405–413
Morrone MC, Di Stefano M, Burr DC (1986) Spatial and temporal properties of neurons of the lateral suprasylvian cortex of the cat. J Neurophysiol 56:969–986
Movshon JA, Thompson ID, Tolhurst DJ (1978a) Spatial summation in the receptive fields of simple cells in the cat's striate cortex. J Physiol (Lond) 283:53–77
Movshon JA, Thompson ID, Tolhurst DJ (1978b) Spatial and temporal contrast sensitivity of neurones in areas 17 and 18 of the cat's visual cortex. J Physiol (Lond) 283:101–120
Munoz DP, Guitton D (1991) Control of orienting gaze shifts by the tectoreticulospinal system in the head-free cat. II. Sustained discharges during motor preparation and fixation. J Neurophysiol 66:1624–1641
Munoz DP, Wurtz RH (1993a) Fixation cells in monkey superior colliculus. I. Characteristics of cell discharge. J Neurophysiol 70:559–575
Munoz DP, Wurtz RH (1993b) Fixation cells in monkey superior colliculus. II. Reversible activation and deactivation. J Neurophysiol 70:576–589
Nagy A, Eördegh G, Benedek G (2003) Spatial and temporal visual properties of single neurons in the feline anterior ectosylvian visual area. Exp Brain Res 151:108–114
Newsome WT, Gizzi MS, Movshon JA (1983) Spatial and temporal properties of neurons in macaque MT. Invest Opthalmol Vis Sci 24(suppl):106
Norita M, Mucke L, Benedek G, Albowitz B, Katoh Y, Creutzfeldt OD. (1986) Connections of the anterior ectosylvian visual area (AEV). Exp Brain Res 62:225–240
Norita M, Kase M, Hoshino K, Meguro R, Funaki S, Hirano S, McHaffie JG (1996) Extrinsic and intrinsic connections of the cat's lateral suprasylvian visual area. Prog Brain Res 112:231–250
Ogasawara K, McHaffie JG, Stein BE (1984) Two visual corticotectal systems in cat. J Neurophysiol 52:1226–1245
Olson CR, Graybiel AM (1987) Ectosylvian visual area of the cat: location, retinotopic organization, and connections. J Comp Neurol 261:277–294
Ouellette BG, Minville K, Faubert J, Casanova C (2004) Simple and complex visual motion response properties in the anterior medial bank of the lateral suprasylvian cortex. Neuroscience 123:231–245
Peck CK, Baro JA (1997) Discharge patterns of neurons in the rostral superior colliculus of cat: activity related to fixation of visual and auditory targets. Exp Brain Res 113:291–302
Perrone JA, Thiele A (2001) Speed skills: measuring the visual speed analyzing properties of primate MT neurons. Nat Neurosci 4:526–532

Perrone JA, Thiele A (2002) A model of speed tuning in MT neurons. Vision Res 42:1035–1051
Pettigrew JD, Cooper ML, Blasdel GG (1979) Improved use of tapetal reflection for eye-position monitoring. Invest Ophthalmol Vis Sci 18:490–495
Pinter RB, Harris LR (1981) Temporal and spatial response characteristics of the cat superior colliculus. Brain Res 207:73–94
Priebe NJ, Cassanello CR, Lisberger SG (2003) The neural representation of speed in macaque area MT/V5. J Neurosci 23:5650–5661
Priebe NJ, Lisberger SG, Movshon JA (2006) Tuning for spatiotemporal frequency and speed in directionally selective neurons of macaque striate cortex. J Neurosci 26:2941–2950
Rodieck RW, Pettigrew JD, Bishop PO, Nikara T (1967) Residual eye movements in receptive-field studies of paralyzed cats. Vis Res 7:107–110
Rowe MH, Cox JF (1993) Spatial receptive-field structure of cat retinal W cells. Vis Neurosci 10:765–779
Saul AB, Humphrey AL (1990) Spatial and temporal response properties of lagged and nonlagged cells in cat lateral geniculate nucleus. J Neurophysiol 64:206–224
Saul AB, Humphrey AL (1992) Temporal-frequency tuning of direction selectivity in cat visual cortex. Vis Neurosci 8:365–372
Schiller PH, Tehovnik EJ (2001) Look and see: how the brain moves your eyes about. Prog Brain Res 134:127–142
Schneider GE (1969) Two visual systems. Science 163:895–902
Schoppmann A, Hoffmann KP (1979) A comparison of visual responses in two pretectal nuclei and in the superior colliculus of the cat. Exp Brain Res 35:495–510
Sireteanu R, Hoffmann KP (1979) Relative frequency and visual resolution of X- and Y-cells in the LGN of normal and monocularly deprived cats: interlaminar differences. Exp Brain Res 34:591–603
Sprague JM (1996) Neural mechanisms of visual orienting responses. Prog Brain Res 112:1–15
Stein BE, Meredith MA (1991) Functional organization of the superior colliculus. In: Leventhal AG (ed) The neural basis of visual function. In: Cronly-Dillon J (series ed) Vision and visual dysfunction, vol 4, Macmillan, London, pp 85–110
Stein BE, Jiang W, Wallace MT, Stanford TR (2001) Nonvisual influences on visual-information processing in the superior colliculus. Prog Brain Res 134:143–156
Sur M, Sherman SM (1982) Linear and nonlinear W-cells in C-laminae of the cat's lateral geniculate nucleus. J Neurophysiol 47:869–884
Tardif E, Bergeron A, Lepore F, Guillemot JP (1996) Spatial and temporal frequency tuning and contrast sensitivity of single neurons in area 21a of the cat. Brain Res 716:219–223
Tardif E, Richer L, Bergeron A, Lepore F, Guillemot JP (1997) Spatial resolution and contrast sensitivity of single neurons in area 19 of split-chiasm cats: a comparison with primary visual cortex. Eur J Neurosci 9:1929–1939
Tardif E, Lepore F, Guillemot JP (2000) Spatial properties and direction selectivity of single neurons in area 21b of the cat. Neuroscience 97:625–634
Tolhurst DJ, Movshon JA (1975) Spatial and temporal contrast sensitivity of striate cortical neurones. Nature 257:674–675
Waleszczyk WJ, Wang C, Burke W, Dreher B (1999) Velocity response profiles of collicular neurons: parallel and convergent visual information channels. Neuroscience 93:1063–1076
Waleszczyk WJ, Nagy A, Eördegh G, Wypych M, Benedek G (2003a) Spatiotemporal frequency response profiles of single neurons in the cat's superior colliculus. Acta Neurobiol Exp 63:255
Waleszczyk WJ, Nagy A, Eördegh G, Wypych M, Benedek G (2003b) Speed tuned cells in feline superior colliculus. Acta Neurobiol Exp 63(suppl):85
Waleszczyk WJ, Wang C, Benedek G, Burke W, Dreher B (2004) Motion sensitivity in cat's superior colliculus: contribution of different visual processing channels to response properties of collicular neurons. Acta Neurobiol Exp 64:209–228
Wang C, Waleszczyk WJ, Benedek G, Burke W, Dreher B (2001) Convergence of Y and non-Y channels onto single neurons in the superior colliculi of the cat. Neuroreport 12:2927–2933
Wurtz RH, Albano JE (1980) Visual-motor function of the primate superior colliculus. Annu Rev Neurosci 3:189–226
Wylie DRW, Crowder NA (2000) The spatio-temporal properties of fast and slow neurons in the pretectal nucleus lentiformis mesencephali in pigeons. J Neurophysiol 84:2529– 2540
Zumbroich TJ, Blakemore C (1987) Spatial and temporal selectivity in the suprasylvian visual cortex of the cat. J Neurosci 7:482–500